STABILITY OF THE WAVE BEARING ON AN ELASTIC SUPPORT

Florin Dimofte and Theo G. Keith, Jr.
The University of Toledo
Toledo, Ohio

ABSTRACT

Numerical computation predicts that an elastic support can substantially improve the stability of the wave bearing if the dynamic stiffness and damping of this support are in a specific range of values. To experimentally validate this prediction, the housing of a gas bearing was mounted on elastic O-rings and the threshold of sub-synchronous whirl motion was experimentally observed when the bearing runs unloaded with a rotating speed up to 30,000 RPM. The O-ring system was also dynamically characterized by measuring its stiffness and damping at various frequencies up to 500 Hz. Good correlation exists between the experimental data and numerical prediction.

1. INTRODUCTION

Fluid film bearings can experience stability problems such as whirl motions of the shaft inside the bearing. The frequency of this motion is, in most cases, equal to or less than one-half of the shaft rotational frequency and is called a "Fractional Frequency Whirl" (FFW). Unloaded plain journal bearings are very susceptible to a FFW. Gas plain journal bearings that experience a FFW usually develop an unstable motion, and wall contact generally occurs immediately after the onset of the whirl motion due to the low damping of the gas film, resulting in bearing failure. This phenomenon was observed soon after gas bearings were applied, starting in the mid-1950's. Due to its importance for bearing life FFW was thoroughly analyzed as a fluid film instability condition. Among others, Castelli and Elrod [1], and Constantinescu [2] contributed work that theoretically established when FFW occurs.

Unlike the plain journal bearing (Fig. 1a), a wave journal bearing reduces the susceptibility to FFW. A wave journal bearing [3] is a bearing with a slight, but precise, variation in the circular profile of the bearing such that a waved profile is circumscribed on the inner bearing diameter. The profile has a wave amplitude that is a fraction of the bearing clearance. Figure 1b, shows a three-wave bearing. The clearance and the wave and the wave amplitude are greatly exaggerated in Figs. 1a and 1b so that the concept may be visualized.

The wave journal bearing capacity to reduce the susceptibility to FFW was demonstrated theoretically in 1993 [3]. A parametric study indicated that the wave journal bearing offers better stability than the plain journal bearing for all operating conditions. However, the wave journal bearing performance is dependent upon the wave amplitude and performance increases significantly as the wave amplitude increases.

Experimental work on gas wave journal bearings validated numerical predictions [4]. It was also demonstrated that an unloaded journal bearing with an altered circular profile, such as a wave bearing, allows operation over a range of speeds under which the bearing can run free of FFW while the plain journal bearing is unstable.

A theoretical correlation between the bearing dynamic behavior and the wave amplitude based on a dimensionless representation of the parameters was presented in ref. [5]. In addition, this work showed that the actual region, in terms of bearing numbers, where the influence of the WAR to the bearing stability is limited. The bearing stability can be controlled well by the WAR if the bearing number, Λ, is less than 10.

However, applications of fluid film gas bearings where they should run at bearings number greater than 10 are very likely to be needed due to a continuous increasing of machine performances. Therefore, an efficient way to increase the bearing stability is to install the fluid film bearing in its housing on an elastic pad that can provide the necessary stiffness and damping in order to stabilize the bearing.

The present report analysis the possibility to further increase the wave bearing stability by using an elastic

bearing pad with dynamic stiffness and damping characteristics. The concept to use an elastic pad in order to stabilize a fluid film bearing was applied, analyzed, and discussed since middle of 60's. Thus, Lund in 1965 [6] made a theoretical analysis to investigate the stability of a symmetrical, flexible rotor supported in journal bearings. He found that when the bearing support possesses damping in addition to flexibility, the speed at onset of instability can be raised significancy above the threshold speed of a rotor in rigidly mounted bearings. Then, Powell in 1967 [7] reported that using pressurized air bearings which are supported by o-rings the speed of a dental turbine could be increased from 250,000 to 500,000 RPM. Marsh reported also 1969 [8], based on a liniearized theory, that for self-acting gas journal bearings additional elements of flexibility in order to improve bearing stability is of considerable practical interest. Boffey stated also in 1969 [9], based on an analytical approach, that given the necessary values of damping and stiffness of the bearing support a self-acting gas journal bearing can run stable at all speeds. In 1971 Tondl [10] reported work on the stability of air-pressurized bearings when a elastically-suspended foundation mass is used. He found that using an elastically suspended foundation mass with damping can, for a suitable tuned foundation mass, sufficient linear foundation damping and proper ratio between the masses and moments of inertia, substantially raise the limit of spontaneous initiation of self-exited vibrations. Elrod and Glanfield presented in 1971 [11] a computer procedure for the design of flexible mounted, externally pressurized gas lubricated journal bearings. Their code predicted that a bearing support with a intermediate values of damping can greatly raise the threshold of bearing instability while at large damping values this threshold drops extremely rapid. Tatara et al. reported in 1973 [12] that whirl on-set speed of flexibly supported, externally pressurized gas journal bearing can be made very high by adequately selecting the dynamic characteristics of the bearing support in relation to the rotor and bearings. This result is also supported by the work reported by Kazimierski and Jarzecki in 1979 [13]. In addition they pointed out some discrepancies between the theory and experiments when o-rings are used as elastic bearing pads due to the evaluation process of the o-ring's dynamic stiffness and damping.

The above review of published information shows that an elastic pad definitely confirm that an elastic pad should improve the bearing stability. However, the dynamic characteristics of this pad should be selected in a specific range that needs to be find for each particularly application [8, 11, and 12]. This aspect will be address through the following analysis that will be focused particularly on the wave bearing. O-rings were selected as elastic bearing pad. Based on [12 and 13] our conclusion was that if o-rings are used their dynamic characteristics should be evaluated over the whole range of frequency they are suppose to work and in the same working condition that is expected they will be used. Therefore, experimental results reported in a comprehensive work on o-ring characteristics such as [14] can be use only informative with precautions and measurements should be made based on the actual application. Thus a special devise was designed and made to measure o-ring dynamic coefficients. To conclude this work experimental tests were conducted to validated this theory.

2. ANALYSIS

The pressure generated in the fluid can be calculated by integrating the Reynolds equation. Assuming a compressible lubricant with isothermal behavior, the Reynolds equation has the following dimensionless form [15]:

$$\frac{\partial}{\theta}\left(h^3\frac{\partial p^2}{\partial\theta}\right) + \frac{\partial}{\partial z}\left(h^3\frac{\partial p^2}{\partial z}\right) = 2\Lambda\frac{\partial(ph)}{\partial\theta} + i4f\Lambda\frac{\partial(p}{\partial} \qquad (1)$$

where:

$$p = \frac{\bar{p}}{p_a},\ \theta = \frac{x_1}{R},\ z = \frac{x_3}{R}, \qquad (2)$$

$$\tau = i\,\nu t,\ (i = \sqrt{-1})$$

$$\Lambda = \frac{6\,\mu\,\Omega}{p_a}\left(\frac{R}{C}\right)^2 \qquad (3)$$

The film thickness, h, is made dimensionless by dividing the film thickness equation of a wave bearing:

$$\overline{h} = C + e\cos\theta + e_w \cos[n_w(\theta + \alpha)] \quad (4)$$

by the radial clearance, C. In Equation 4 n_w is the number of waves, α is the angle between the starting point of the wave and the line of centers, and θ is the angular coordinate starting from the line of centers.

The bearing number, Λ (Eq. 3), is the main working parameter of the bearing. It incudes: the dynamic viscosity of the fluid, μ, the ambient operating pressure, p_a, the rotational speed of the shaft, Ω, and the bearing main geometry parameter, (R/C).

2.1 Bearing Steady-State and Dynamic Performance.

The bearing steady-state and dynamic performance can be determined by using the small perturbation technique on the complex form of the Reynolds equation (Eq. 1) [15]. Expanded in a Taylor series truncated to the first derivatives, the pressure can be written as:

$$p = p_0 + \epsilon_1 \exp(\tau)\, p_1 + \epsilon_0\varphi_1 \exp(\tau)\, p_2, \quad (5)$$

where p_0 is the steady-state component and p_1 and p_2 are the dynamic components of the pressure. Each component can be calculated by numerically integrating the corresponding differential equation derived from the Reynolds equation (Eq. 1).

The bearing steady-state and dynamic characteristics can be obtained by integrating the pressure components, p_0, p_1, and p_2, over the whole bearing fluid film. The steady-state load capacity, F, is calculated by integrating p_0, while both the dynamic stiffness, K_{jk}, and damping, B_{jk} (j =x,y; k = x,y), coefficients are calculated by integrating the dynamic pressure components, p_1 and p_2.

2.2 Bearing dynamic reaction force.

Under dynamic conditions, the journal (shaft) center whirls in an orbit around its static equilibrium position. The corresponding bearing dynamic reaction force is actually a nonlinear function of the whirl amplitude and depends implicitly on time. In a thorough analysis it is necessary to consider the rotor and the bearing simultaneously. In most practical situations, the amplitude of the shaft whirl is, of necessity, rather small. In these cases a linearization of the bearing reaction force is permissible [15]. Then, it becomes possible to treat the bearing separately and represent the bearing reaction force components by the means of bearing dynamic coefficients:

$$F_x = -K_{xx}x - B_{xx}\frac{dx}{dt} - K_{xy}y - B_{xy}\frac{dy}{dt}$$

$$F_y = -K_{yx}x - B_{yx}\frac{dx}{dt} - K_{yy}y - B_{yy}\frac{dy}{dt} \quad (6)$$

Equation (Eq. 6) is only valid when the journal motion is harmonic, and:

$$x = \overline{x}\exp(i\nu t) = \overline{x}\exp(\tau)$$

$$y = \overline{y}\exp(i\nu t) = \overline{y}\exp(\tau) \quad (7)$$

The equation (Eq. 6) can be written in complex form as:

$$F_x = -Z_{xx}x - Z_{xy}y$$

$$F_y = -Z_{yx}x - Z_{yy}y \quad (8)$$

where:

$$Z_{jk} = K_{jk} + i\,\nu\,B_{jk} \qquad (9)$$

$$j = (x,y); \quad k = (x,y)$$

are the bearing impedance coefficients. For a given bearing geometry, the dynamic coefficients are functions of the static load on the bearing and the rotor speed. The dynamic coefficients also depend on the whirl frequency, and they are actually impedances of the gas film. Note, also, that the x-axis was chosen along the direction of the steady-state load.

2.3 Bearing Stability.

In a bearing stability calculation, it is necessary to evaluate the bearing coefficients over a frequency range, usually around one half of the rotating frequency. On this basis, a stability analysis can be performed in order to calculate the critical mass. The critical mass, M_c, is used to help determine whether the bearing will run free of FFW. FFW is an instability of the fluid lubricant film of the bearing. It appears as a whirling, orbiting motion of the shaft and its frequency or speed, ν_0, is often close to one-half the running frequency or shaft speed especially if the bearing is unloaded. This phenomenon is more likely to occur when the shaft center is close to the center of the bearing (near zero eccentricity). This frequency, ν_0, can be much lower than one-half of the running frequency when the value of eccentricity is large [16]. To derive the equation for critical mass, in a simple manner, the rotor is considered rigid and symmetrical, and supported by two identical bearings [15]. This means that each bearing carries one-half of the rotor mass. If M is the rotor mass supported by the each bearing (M = ½ of the rotor mass) and the bearing is represented by its four impedance coefficients, $Z_{jk} = K_{jk} + i\nu B_{jk}$ (j = x,y; k = x,y), the motion equation can be written as:

$$\begin{bmatrix} (Z_{xx} - M\,\nu^2) & Z_{xy} \\ Z_{yx} & (Z_{yy} - M\,\nu^2) \end{bmatrix} \begin{bmatrix} x \\ y \end{bmatrix} = 0 \qquad (10)$$

The threshold of instability occurs when the determinant of the matrix is zero. Noting:

$$Z = K_c + i\,\nu\,B_c, \quad K_c = M\,\nu^2 \qquad (11)$$

the determinant equation can be solved to get:

$$Z = \frac{1}{2}\,(Z_{xx} + Z_{yy}) - \sqrt{\frac{1}{4}\,(Z_{xx} - Z_{yy})^2 + Z_{xy}\,Z_{yx}} \qquad (12)$$

For stability calculations only the solution with a negative sign in front of the square root proves to be of interest [15]. At the threshold of instability, Z must be real. The imaginary part of Z can be evaluated over a range of frequencies to find the frequency value, ν_0, causing the imaginary part of Z to be zero. The corresponding mass, is the mass required to make the bearing unstable under the selected working conditions and is:

$$M_c = \frac{K_{c0}}{\nu_0^2} \qquad (13)$$

This critical bearing mass is a threshold and there are three possibilities: I) the critical mass is positive which means that the bearing could run stably if its actual allocated mass is less that the critical mass; ii) the threshold of instability was not found and the critical mass can be considered infinite which means that the bearing could run stably at any value of its actual allocated mass; iii) the critical mass is negative which means that the half frequency whirl instability is most likely to occur for any value of the rotor mass. The actual allocated mass is half of the rotor mass.

2.4 Effect of the bearing support stiffness and damping on bearing stability.

When bearing is supported by an elastic pad that has dynamic stiffness, K_p, and damping, B_p, and between the

bearing fluid film and the elastic support there is an intermediate mass, m_p, the motion equation (10) becomes:

$$\begin{bmatrix} (Z_{xx} - M\nu^2 - A_{p1}) & Z_{xy} - A_{p2} \\ Z_{yx} - A_{p3} & (Z_{yy} - M\nu^2 - A_{p4}) \end{bmatrix} \begin{bmatrix} x \\ y \end{bmatrix} = 0 \qquad (14)$$

where A_{p1}, A_{p2}, A_{p3}, and A_{p4} are functions of bearing impedance , Z_{ij}, the elastic pad impedance , $Z_p = K_p + i\nu B_p$, and the intermediate mass, m_p. If the bearing sleeve is just elastically supported the intermediate mass is the sleeve mass.

At the threshold of instability Z from expression (11) must be real. Therefore scanning down frequencies up to the value ν_0 where the imaginary part of Z is vanished, the real part of Z (equation 12) becomes:

$$K_c = M_c\nu_0^2 = 0.5\left[(Z_{xx}-A_{p1}) + (Z_{yy}-A_{p4})\right] - \left\{0.25\left[(Z_{xx}-A_{p1}) + (Z_{yy}-A_{p4})\right]^2 - \left[(Z_{xx}-A_{p1})(Z_{yy}-A_{p4}) - (Z_{yx}-A_{p3})(Z_{xy}-A_{p2})\right]\right\}^{\frac{1}{2}} \qquad (15)$$

and the critical mass can be again calculated by using equation (13).

2.5 Numerical Results.

Calculations were performed on the stability of a 35 mm diameter and 30 mm long gas journal bearing. The bearing radial clearance was 16 microns. The bearing was considered unloaded. Both a true circular and a three wave bearing geometry were analyzed. The wave bearing had a wave amplitude ratio of 0.3. The bearing was considered mounted on an elastic support. The support stiffness was varied from 10 to 10^7 N/m and the support damping was varied from 10 to 1000 Ns/m. The critical mass values that show the limits of bearing stability are listed in Tab. 1 and 2. The results of a rigid supported bearing are also listed in an additional column for comparison purpose.

In Tab.1 stability data of the true circular journal bearing are listed. This data shows that a true circular bearing rigidly supported is unstable at any analyzed speed from 3,000 to 30,000 RPM. Supporting the bearing into an elastic pad can help in order to stabilize the bearing if the stiffness and damping of the elastic pad are properly selected. Thus, for example, if K_p = 10 to 10,000 N/m and B_p = 100 Ns/m, the true circular bearing can run unconditionally stably up to 15,000 RPM. Both lower and higher stiffness and damping values than that listed above keep the bearing unstable.

Tab. 2 shows the critical mass value for a similar journal bearing as the true circular but this bearing had three waves with a wave amplitude ratio of 0.3. This bearing mounted rigidly, unlike the true circular bearing, can run stable if the rotor mass is less then the critical mass listed in Tab. 2 in the column called "rigid". However, this stable running condition is rotor mass depended and the threshold of stably running condition (the critical mass) is diminishing progressively while speed increases. At 3,000 RPM the critical mass is 2.12 kg while at 30,000 RPM is only .774 kg. Therefore at higher speeds the critical mass, still positive, could have very small values that has not any practical interest. Looking to all data listed in Tab. 2 it can be seen that supporting the bearing into an elastic pad with K_P = 10 to 100,000 N/m and B_p = 100 to 1000 Ns/m it can run unconditionally stably at all analyzed speeds. In other words no restriction is imposed to the rotor mass in order to run the bearing stably. Therefore supporting a wave bearing on an elastic pad with properly selected stiffness and damping make a substantial improvement in bearing overall stability.

3. EXPERIMENTAL WORKS

In order to validate the theory and to established the procedure how to use the O-rings as a elastic bearing support experimental works were conducted in two main direction:
1. Evaluation of o-rings dynamic characteristics, and
2. Test the effect of the o-rings on bearing stability.

3.1 Evaluation of O-rings dynamic stiffness and damping.

A measuring devise was designed and manufactured to measure the dynamic stiffness and damping of the o-rings for elastic pad. This devise is shown in Fig. 2a. A Piezo-shaker provided sine strokes into 1 to 5 microns amplitude range with frequencies up to 500 Hz. A dynamic load cell and a proximity probe read the load and the displacement, respectively. Small stroke amplitudes were used in order to know the o-ring characteristics just close to the moment when the instability starts. At that moment the shaft inside the bearing whirls with very small orbits. This approach make the comparison between the theory and the experiment consistent because this theory predicts the moment when the instability starts base on "a small perturbation technique". Based on this analysis it can be known what to do to avoid a FFW and to run the bearing stably. What happened inside the bearing when shaft is whirling with more or less large orbit could be a subject of an other type of analysis such as a transient analysis.

Both load cell and proximity probe signals can be seen superposed on a oscilloscope screen. Pictures at 10 Hz and 400 Hz of this screen are presented in Fig. 2 b and c, respectively. The scope can display the frequency and the amplitude among other information. Comparing Fig 2 b and c it can be easy seen that increasing the frequency the diphase between the force and the displacement increases. The displacement is after the force due to the damping of the system.

Measured stiffness and damping for various o-ring configuration are presented in Figs. 3 to 6. Measurements were performed at frequencies form 50 to 500 Hz. The used o-rings have these basic catalog dimensions: mean diameter = 2.125" (53.975 mm) and thickness = 0.070" (1.778 mm) and they are in "sealing o-ring specification". However, it was found that when they are used as an elastic gas bearing support a precompression of these o-rings form .070" to .050" is too large and make the o-rings too stiff. Therefore, a precompression from .070" to .060" was only used.

In Fig. 3 a and b the measured stiffness and damping, respectively, for 2, 3, 4, and 5 nitril o-rings used to support the bearing sleeve are shown and difference in stiffness and damping can be seen as is expected. However, a big jump in dynamic characteristics can be observe when 5 0-rings were used compared to the other o-ring configurations.

Fig. 4 shows the dynamic characteristics of a bearing elastic pad of two nitril o-rings that have the shore hardness 50, 70, 80, and 90. The results are as expected, at an increase in shore hardness both stiffness and damping increase.

In Fig. 5 the stiffness and damping of fluorosilicone and ethylene propylene o-rings can be compared. This figure shows that same dimension and hardness O-rings but from different materials show different dynamic properties. More of this, "same" 0-ring material but made by different manufactures lead also in significant differences in O-ring dynamic properties as it is shown in Fig. 6.

Reviewing all this data the main conclusion is that the o-rings produced under a "sealing specification" should be sorted and measured for each specific application. Their dynamic properties could vary in a unacceptable range for elastic pad application if they are not sorted. Their dynamic characteristics should be evaluated by simulating all working condition and over the whole range of working frequencies.

3.2 Test of the effect of the o-rings on bearing stability.

Experimental evaluations of O-ring effect on the bearing stability were conducted by using an experimental bearing with 35 mm diameter, 30 mm long, and 18 microns radial clearance. This bearing had three wave with 0.3 wave amplitude ratio. Fig. 7 show the picture of this bearing. In this case, the waved bearing sleeve is mounted inside a bearing

housing. The whole bearing housing assembly has a mass of 0.276 kg. On the housing outer surface there are four grooves where the o-rings could be mounted. In order to run this bearing on the wave bearing rig, well described in references [ ] an adequate test bearing assembly was designed and fabricated (Fig. 8) The upper and the bottom faces of the housing (Fig.8 #1) are supported by two thrust pressurized air bearing plates so that this housing moves freely in the horizontal plane while it is very well positioned in the vertical and angular directions. Two holes at 90 degrees made in the housing were used to fix two proximity probes that red the movement between the housing and the shaft (Fig. 7 #4). For these tests sets of two nitril o-rings were used. The o-rings shore hardness were 50, 70, 80, and 90. The shaft was turned at various speeds up to the speed when the FEW just started to install.

Typical oscilloscope screen pictures are shown in Fig. 9. The scope spot visualized the vibration of the housing, in regards to the shaft, in one direction. Pictures in Fig. 9 were made when two nitric o-rings with 50 shore hardness were used to support the bearing inside the housing. When the bearing run stably, the scope screen looks like in Fig. 9 a. Only synchronous vibration with a few microns amplitude can be observed due to a small shaft-bearing rotor runout. The frequency red by the scop (91.74 Hz) corresponded to the running speed of 5,504 RPM. At the instability threshold the scop screen started to display the changing in vibration as can be seen in Fig. 9 b. Actually, the curve started to "dance" the vibration period was doubling and the frequency red by the scop (57.47 Hz) was almost half of the synchronous frequency that corresponded to a rotation speed of 6,840 RPM.

In order to promptly observe the effect of the o-rings on bearing stability an additional test was performed. The housing (Fig.8 #1) was provided with three radial screws that can seize the bearing (Fig. 8 #2) vanishing the o-rings effect. Thus, the shaft started rotating and the speed was increased to 1,153 RPM. The bearing was supported by two nitric o-rings with 90 shore hardness and run stably. The scope screen looked like in Fig. 10 a. Only a synchronous vibration was detected. Then, the screws were tightened and the bearing was seized solid to the housing. The FEW installed immediately with large amplitude as can be seen in Fig. 10 b This test definitely proving the o-ring effect to bearing stability.

A comparison of the experimental results to the prediction can be seen in the following table where the observed and predicted threshold speed (RPM) to unstable running condition are listed for various o-ring sets.

Shore Hardness	50	70	80	90
Observed	6,840 RPM	12,500 RPM	11,700 RPM	8,000 RPM
Predicted	6,000-9,000 RPM	9,000-12,000 RPM	9,000-12,000 RPM	9,000-12,000 RPM

The above table shows a reasonable correspondence between the experiment and the prediction.

CONCLUSIONS:

A theoretical analysis was developed to predict the effect of and elastic bearing pad, with dynamic stiffness and damping, on the bearing (fluid film) FEW instability. Then, experimental investigations were conducted in order to evaluate the dynamic stiffness and damping of various elastomer 0-rings used as elastic pads. The experimental work concluded with tests of a wave journal bearing stability when it was supported by o-rings. The conclusions are:

1. The amount of the elastic support stiffness and damping that the bearing needs to run stably can be predicted. The predictions were experimentally verified.

2. The stability of a wave journal bearing can be significantly increased by using an elastic pad unlike the stability of a circular bearing that has a limited possibility to be improved by using an elastic pad. The wave bearing can run unconditional stably over a large range of speeds.

3. The elastic bearing support could be rubber, or any kind of elastomer, 0-rings if the dynamic stiffness and damping of this support are in the predicted range of needed values.

4. The dynamic characteristics of the o-ring are a function of its material, manufacture, precompression and working conditions. Therefore the dynamic stiffness and damping of a specific elastic system based on o-rings have to be measured by simulating the bearing running condition.

5. A method to precisely, dynamically characterize the o-ring elastic system has developed and successfully used.

6. O-rings made in "sealing specification" can be used but with precaution. The o-rings should be sorted by material, manufacture, shore hardness, dimensions, etc, and than each lot should me measured in order to verify the o-ring dynamic characteristics.

ACKNOWLEDGMENTS

This paper reports work conducted at the NASA Lewis Research Center in Cleveland Ohio sponsored under grant NAG awarded to the University of Toledo. The author would like to express his thanks to Dr. John J. Coy, and Margaret from NASA LeRC who all kindly supported this work.

REFERENCES

1. Castelli, V. and Elrod, H.G., "Solution of the Stability Problem for 360 Deg Self-Acting, Gas-Lubricated Bearings," *Journal of Basic Engineering*, Trans. ASME, Series D, Vol. 87, 1, pp. 199-212, (1965).

2. Constantinescu, V.N., "On Hydrodynamic Instability of Gas-lubricated Journal Bearings," *Journal of Basic Engineering*, Trans. ASME, Series D, Vol. 87, 3, pp. 579-588, (1965).

3. Dimofte, F., "Wave Journal Bearing with Compressible Lubricant; Part I: The Wave Bearing Concept and a Comparison with a Plain Circular Journal Bearing", presented to STLE 1993 Annual Meeting, May 17-20, 1993, Calgary, Canada, published in *STLE Tribology Transactions* Vol. 38 1, pp. 153-160, (1995).

4. Dimofte, F., and Hendricks, R.C., "Fractional Whirl Motion in Wave Journal Bearings" presented at The Fourth Seal Code Development Workshop held at NASA Lewis Research Center in Cleveland, Ohio, on June 14-15, 1995, NASA CP 10181, pp. 337-340.

5. Dimofte, F. and Keith, T.G, Jr., " Wave Bearing Technology to Control Journal Bearing Dynamics" in Proceedings of the 7th International Symposium on Transport Phenomena and Dynamics of Rotating Machinery - ISROMAC-7, held on 22-26 Feb. 1998 in Honolulu, Hawaii, Vol 1, pp. 327-336.

6. Lund, J.A. "The Stability of an Elastic Rotor in Journal Bearings With Flexible, Damped Supports.", *Journal of Applied Mechanics*, Trans. ASME, Series , Vol. , 4, pp. 911-920, (1965).

7. Powell, J.W., "A review of the Experience of Producing over 20,000 Air Bearing Dental Turbines", Proceedings of Gas Bearing Symposium, Paper 10, University of Southampton, April 1967.

8. March, H., "The Stability of Self-Acting Gas Journal Bearings With Noncircular Members and Additional Elements of Flexibility",

9. Boffey, D.A., "The Stability of a Rigid Rotor ib a Flexibly Supported Self-Acting Gas Journal Bearing", Proceedings of Gas Bearing Symposium, Paper 12, University of Southampton, April 1969.

10. Tondl, A., "The Effect of an Elastically-Suspended Foundation Mass and Its Damping on the Initiation of Self-Exited

Vibrations of a Rotor Mounted in Air-Pressurized Bearings", Proceedings of Gas Bearing Symposium, Paper 1, University of Southampton, March 1971.

11. Elrod, H.G. and Glanfield G.A. "Computer Procedures for the Design of Flexible Mounted, Externally Pressurized, Gas Lubricated Journal Bearings", Proceedings of Gas Bearing Symposium, Paper 22, University of Southampton, March 1971.

12. Tatara, A., Koike, H., and Iwasaki, A., "The Stability of Flexible Supported, Externally Pressurized Gas Journal Bearings", Bulletin of the JSME, Vol. 100, pp. 1573-1579, Oct. 1973.

13. Kazimierski, Z. and Jarzecki, K., "Stability Threshold of Flexibly Supported Hybrid Gas Journal Bearings", *Journal of Lubrication Technology*, Trans. ASME, Series F, Vol. 101, 3, pp. 451-457, (1979).

14. Darlow, M. and Zorzi, E.,"Mechanical Design Handbook for Elastomers", NASA CR 3423 - 1981

15. Lund, J.W., "Calculation of Stiffness and Damping Properties of Gas Bearings", *Trans. of ASME, Journal of Lubrication Technology*, Series F, 90, 4, pp. 793-808, (1968).

16. Dimofte, F., "Effect of Fluid Compressibility on Journal Bearing Performance," *STLE Tribology Transactions* Vol. 36, 3, pp. 341-350, (1993).

TABLE 1

Critical Mass (kg) or Stability Criteria of a True Circular Bearing with D = 35 mm, L = 30 mm, C = 0.016 mm, Sleeve Mass=0.276 kg.										
Speed RPM	RIGID	K_p = 10 N/m	10	10	1,000	1,000	1,000	10,000	10,000	10,000
		B_p = 10 Ns/m	100	1,000	10	100	1,000	10	100	1,000
3,000	unstable	STABLE	STABLE	unstable	STABLE	STABLE	unstable	STABLE	STABLE	STABLE
6,000	unstable	unstable	STABLE	unstable	STABLE	STABLE	unstable	STABLE	STABLE	unstable
9,000	unstable	STABLE	STABLE	unstable	STABLE	STABLE	unstable	unstable	STABLE	unstable
12,000	unstable	STABLE	STABLE	unstable	STABLE	STABLE	unstable	STABLE	STABLE	unstable
15,000	unstable	unstable	STABLE	unstable	unstable	STABLE	unstable	STABLE	STABLE	unstable
18,000	unstable	unstable	unstable	unstable	unstable	unstable	unstable	unstable	unstable	unstable
21,000	unstable	unstable	unstable	unstable	unstable	unstable	unstable	unstable	unstable	unstable
24,000	unstable	STABLE	unstable	unstable	STABLE	unstable	unstable	unstable	unstable	unstable
27,000	unstable	STABLE	STABLE	unstable	STABLE	STABLE	unstable	STABLE	STABLE	unstable
30,000	unstable	STABLE	STABLE	unstable	STABLE	STABLE	unstable	STABLE	STABLE	unstable

TABLE 1 Cont.

Critical Mass (kg) or Stability Criteria of a True Circular Bearing with D = 35 mm, L = 30 mm, C = 0.016 mm, Sleeve Mass=0.276 kg.									
Speed RPM		K_p =100,000 N/m	100,000	100,000	1,000,000	1,000,000	1,000,000	10,000,000	10,000,000	10,000,000
		B_p = 10 Ns/m	100	1,000	10	100	1,000	10	100	1,000
3,000		unstable	unstable	STABLE	unstable	unstable	unstable	unstable	unstable	unstable
6,000		unstable	STABLE	STABLE	unstable	unstable	unstable	unstable	unstable	unstable
9,000		unstable	STABLE	STABLE	unstable	unstable	unstable	unstable	unstable	unstable
12,000		STABLE	STABLE	STABLE	unstable	unstable	unstable	unstable	unstable	unstable
15,000		STABLE	STABLE	unstable	unstable	unstable	unstable	unstable	unstable	unstable
18,000		STABLE	STABLE	unstable	unstable	unstable	unstable	unstable	unstable	unstable
21,000		STABLE	unstable	unstable	unstable	unstable	unstable	unstable	unstable	unstable
24,000		STABLE	unstable	unstable	unstable	unstable	unstable	unstable	unstable	unstable
27,000		unstable	unstable	unstable	unstable	unstable	STABLE	unstable	unstable	unstable
30,000		unstable	unstable	unstable	unstable	STABLE	STABLE	unstable	unstable	unstable

TABLE 2 Cont.

Critical Mass (kg) or Stability Criteria of a Wave BRG with WAR = 0.3, D = 35 mm, L = 30 mm, C = 0.016 mm, Sleeve Mass=0.276 kg.										
Speed RPM		K_p=100,000 N/m	100,000	100,000	1,000,000	1,000,000	1,000,000	10,000,000	10,000,000	10,000,000
		B_p = 10 Ns/m	100	1,000	10	100	1,000	10	100	1,000
3,000		1.360	1.396	STABLE	2.014	2.014	2.018	2.109	2.109	2.109
6,000		0.554	STABLE	STABLE	1.613	1.616	1.666	1.893	1.893	1.893
9,000		0.337	STABLE	STABLE	1.235	1.244	1.414	1.677	1.678	1.679
12,000		0.974	STABLE	STABLE	0.925	0.945	1.322	1.465	1.465	1.468
15,000		1.890	STABLE	STABLE	0.691	0.725	STABLE	1.275	1.273	1.277
18,000		3.084	STABLE	STABLE	0.516	0.571	STABLE	1.105	1.105	1.111
21,000		4.599	STABLE	STABLE	0.386	0.469	STABLE	0.962	0.962	0.970
24,000		unstable	STABLE	STABLE	0.287	0.414	STABLE	0.840	0.841	0.850
27,000		unstable	STABLE	STABLE	0.212	0.425	STABLE	0.737	0.738	0.749
30,000		unstable	STABLE	STABLE	0.157	0.515	STABLE	0.649	0.650	0.662

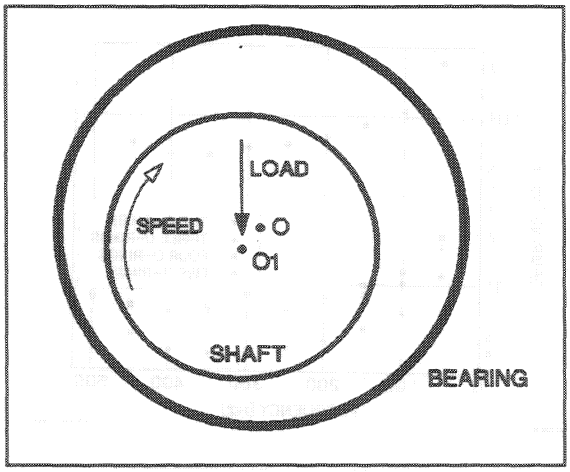

a. True Circular

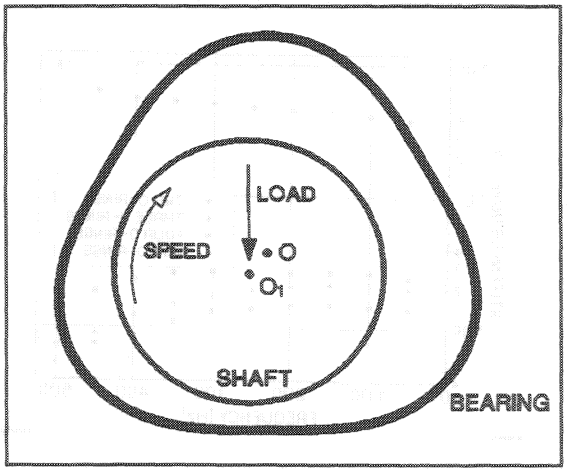

b. Three Wave

Fig. 1 Journal Bearing

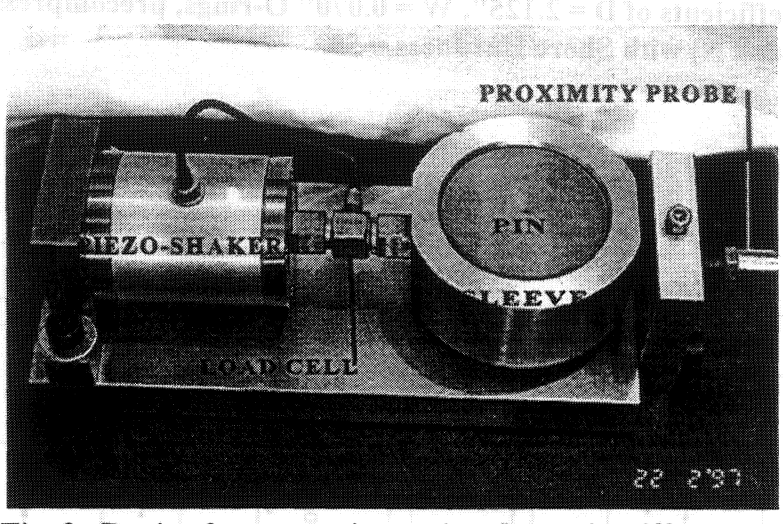

Fig. 2a Device for measuring o-ring dynamic stiffness and damping

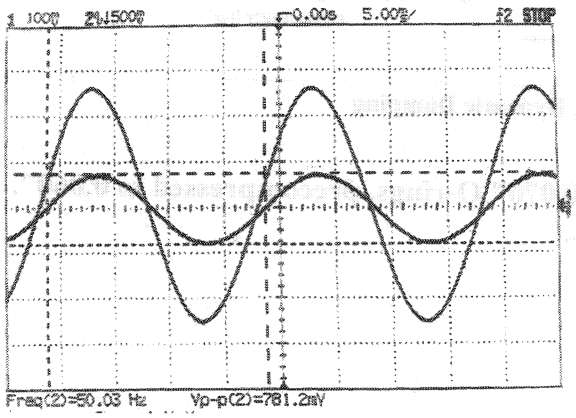

Fig. 2b Force & Displacement at 50 Hz.

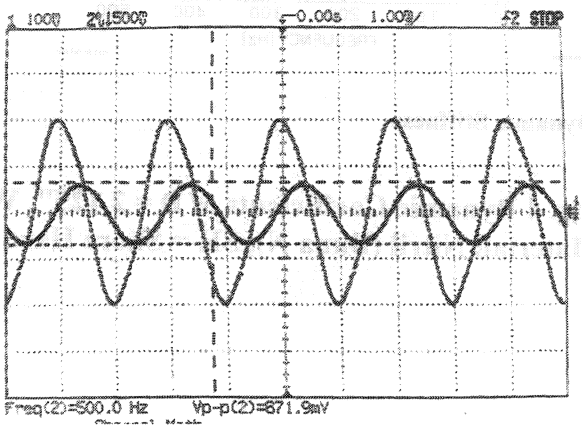

Fig. 2c Force & Displacement at 500 Hz.

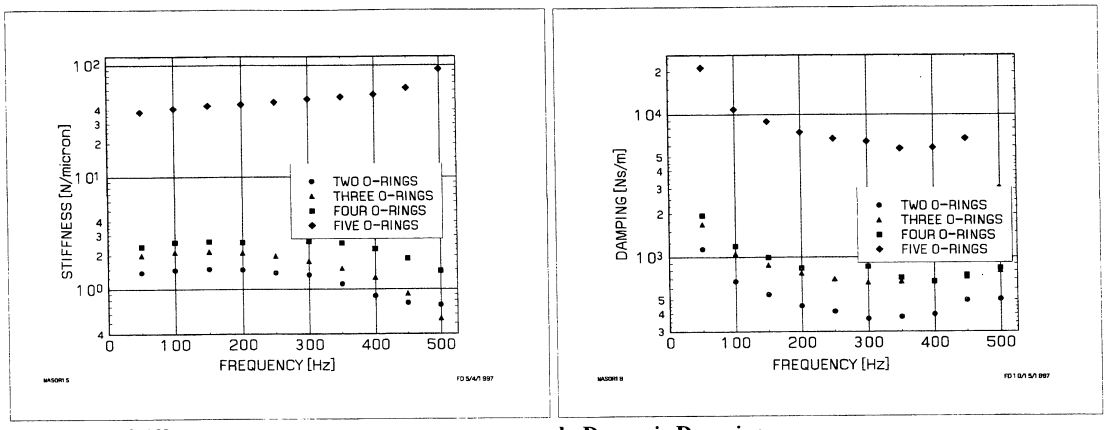

a. Dynamic Stiffness

b. Dynamic Damping

Fig. 3 Dynamic Coefficients of D = 2.125", W = 0.070" O-rings, precompressed to 0.060". Material: Nitril (Buna N) with Shore Hardness = 50.

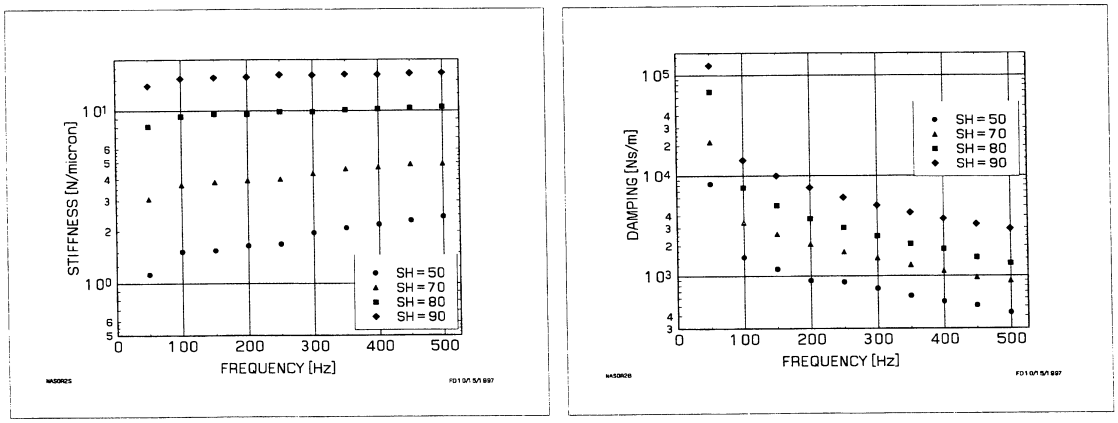

a. Dynamic Stiffness

b. Dynamic Damping

Fig. 4 Dynamic Coefficients of D = 2.125", W = 0.070" O-rings, precompressed to 0.060". Material: Nitril (Buna N), SH = Shore Hardness.

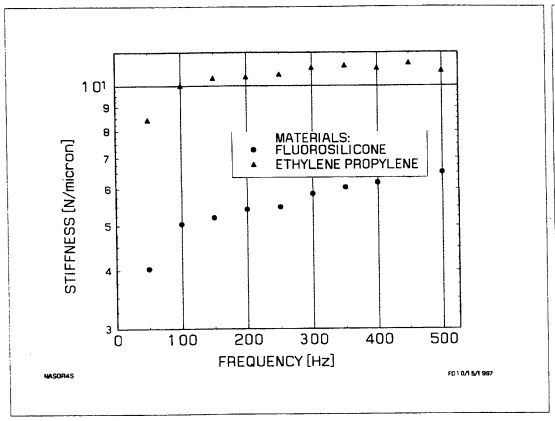

a. Dynamic Stiffness

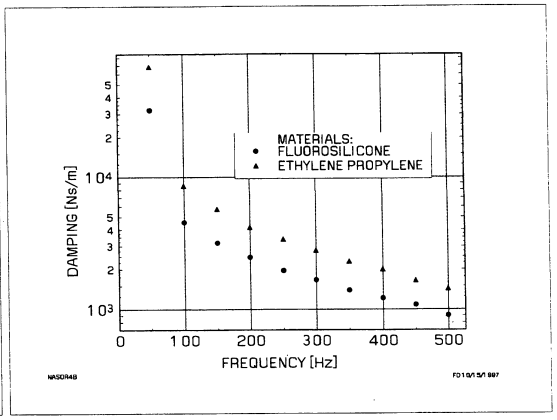

b. Dynamic Damping

Fig. 5 Dynamic Coefficients of D = 2.125", W = 0.070" O-rings, precompressed to 0.060". Shore Hardness = 80.

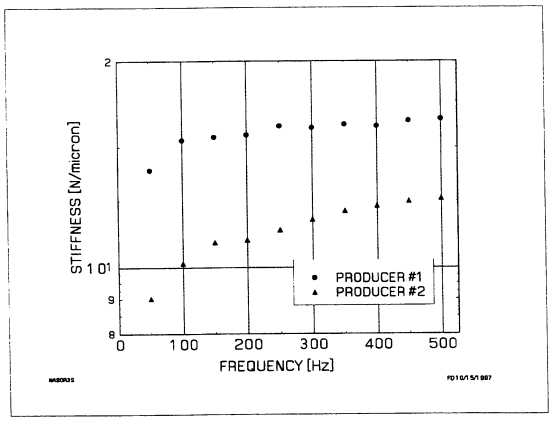

a. Dynamic Stiffness

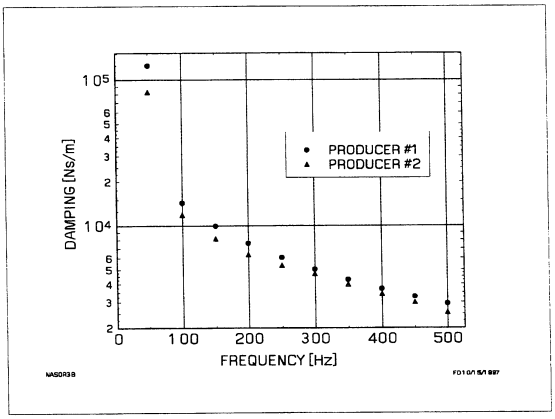

b. Dynamic Damping

Fig. 6 Dynamic Coefficients of D = 2.125", W = 0.070" O-rings, precompressed to 0.060". Material: Nitril (Buna N), Shore Hardness = 90.

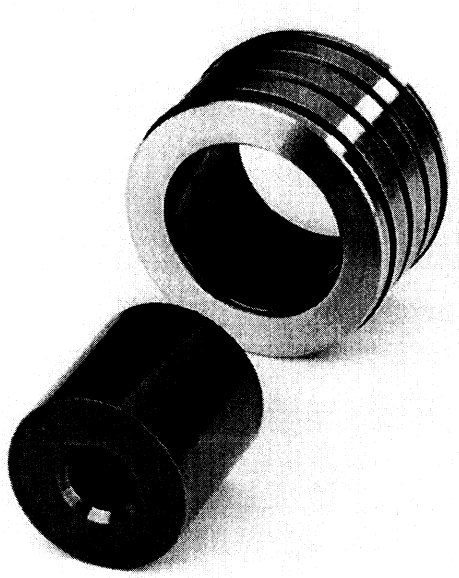

Fig. 7 Test Bearing, Rotor and Sleeve Assembly

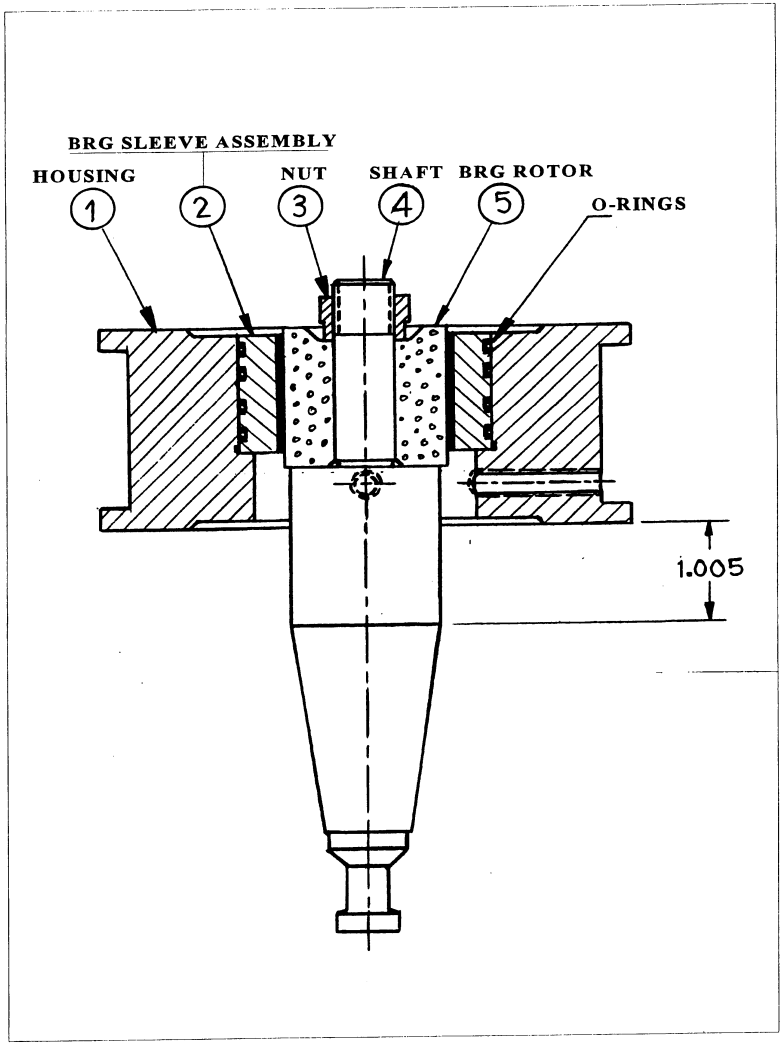

Fig. 8 Test Bearing Assembly

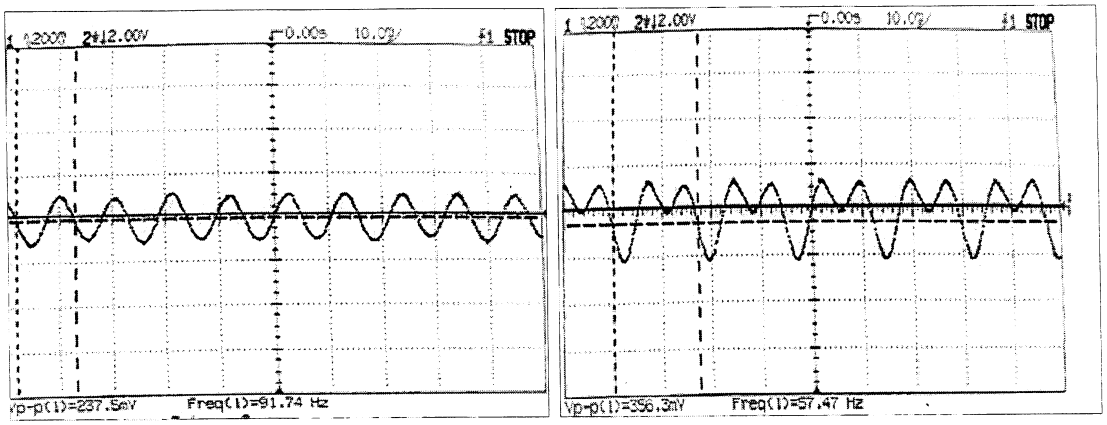

a. Stable at 5,504 RPM

b. Unstable at 6,840 RPM

Fig. 9 Stability Threshold of the Test Bearing when It Is Supported by 2 Buna O-rings with Shore Hardness = 50.

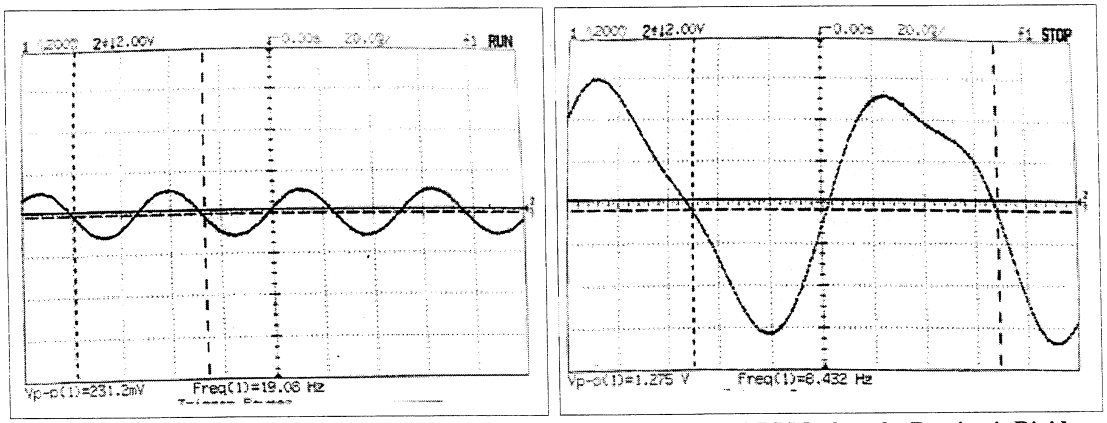

a. Stable at 1,153 RPM when the Bearing is Supported by 2 Buna O-rings with Shore Hardness = 90.

b. Unstable at 1,153 RPM when the Bearing is Rigid Mounted in the Housing.

Fig. 10 Stability of a Wave Bearing when It is Supported by O-rings or It is Rigid Mounted into the Housing.